Lasers in Surgery and Medicine 9:314–326 (1989)

Er:YAG Laser Ablation of Tissue: Effect of Pulse Duration and Tissue Type on Thermal Damage

Joseph T. Walsh, Jr., PhD, Thomas J. Flotte, MD, and Thomas F. Deutsch, PhD

Wellman Laboratories, Department of Dermatology, Massachusetts General Hospital, Boston, Massachusetts 02114

The thermal damage caused by 2.94-μm Er:YAG laser ablation of skin, cornea, aorta, and bone was quantified. The zone of residual thermal damage produced by normal-spiking-mode pulses (pulse duration ≈ 200 μs) and Q-switched pulses (pulse duration ≈ 90 ns) was compared. Normal-spiking-mode pulses typically leave 10–50 μm of collagen damage at the smooth wall of the incisions; however, at the highest fluences (≈ 80 J/cm^2) tears were produced in cornea and aorta and as much as 100 μm of damaged collagen is found at the incision edge. Q-switched pulses caused less thermal damage, typically 5–10 μm of damage in all tissues.

Key words: skin, cornea, aorta, bone, tissue denaturation, tissue damage, modeling

INTRODUCTION

The continuous wave (cw) CO_2 laser has long been used in medicine and surgery to incise tissue [1]. The great advantage of this laser over the scalpel is that a cut made with the CO_2 laser can be relatively hemostatic. Hemostasis is achieved because the laser leaves several hundred microns of thermally coagulated tissue at the cut edge. The disadvantage of this type of incision is that the body must deal with the damaged tissue. Typically, the coagulated tissue is sloughed; however, entrapment of the coagulum has been noted [2]. The healing of CO_2 laser cuts is often slower than scalpel cuts, and scar formation can be clinically unsatisfactory [3–5]. There are instances when precise removal of tissue is required, and large zones of damage and subsequent scarring may not be tolerated, for example, in corneal surgery and skin grafting [6–8]. It is expected that short pulses of strongly absorbed infrared laser radiation can be used to ablate tissue and leave a minimal zone of damaged tissue at the ablation crater edge.

It has been shown, using a CO_2 laser, that if the laser pulse duration is less than the thermal relaxation time of the initially laser-heated layer of tissue, then the zone of damage is minimized [9]. To further decrease the zone of damage, a laser is needed that emits radiation more strongly absorbed than CO_2 laser radiation; the absorption coefficient of water, α, at 10.6 μm is approximately 790 cm^{-1}; thus, $1/\alpha \approx 13$ μm [9–12]. Incisions with little residual thermal damage have been demonstrated with 193-nm excimer laser pulses [13–15]. In cornea, the absorption coefficient at 193 nm is 2,700 cm^{-1}, and the damage zones can be less than 1 μm wide [15]. Similar results are expected using a laser that emits in the infrared at the 2.94-μm peak of the water absorption spectrum at which the absorption coefficient of pure water is approximately 13,000 cm^{-1} [10–12]. In tissue, which is typically 70% water, the optical penetration depth, $1/\alpha$, should be approximately 1 μm. For clinical use, the major advantages of 2.94-μm radiation over UV excimer laser radiation are: 1) there are no known mutagenic or carcinogenic effects of infrared radiation [16]; and 2) the solid-state

Accepted for publication April 10, 1989.

Address reprint requests to Dr. Joseph T. Walsh, Jr., Department of Biomedical Engineering, Technological Institute, Northwestern University, 2145 Sheridan Road, Evanston, IL 60208.

Er:YAG laser system is less expensive and more compact than the excimer laser system.

The advantages of 2.94-μm radiation for tissue ablation have been discussed [17]; subsequent brief reports indicated that 2.94-μm radiation from an Er:YAG laser can effectively cut a variety of tissues, leaving thin zones of thermally-damaged tissue [18–20]. Bonner et al. found 3–10 μm of damage at the ablation crater edge in cadaveric artery and bone, a result consistent with a simple thermal damage model [21]. More recent reports have demonstrated that normal-spiking-mode Er:YAG laser radiation can effectively cut bone and leave between 5 and 10 μm of damage [22,23].

We present a systematic comparison of the effect of laser pulse duration on residual thermal damage in four different tissues. Because of the short penetration depth of the 2.94-μm radiation, the laser-heated layer of tissue is initially 1 μm wide and has a thermal relaxation time of approximately 1 μs [9,17,24]. Single pulses less than 1 μs in duration are needed to minimize thermal diffusion during the laser pulse and therefore minimize the zone of thermal damage. None of the above groups used pulses less than 1 μs in duration. Other groups, however, have reported ablation with short pulses of radiation near the 3 μm water absorption peak. Seiler et al. used 50-ns-long pulses from a multiline hydrogen fluoride (HF) laser to ablate cornea [25]. These authors found that at 140 mJ/cm^2, the maximum fluence achievable with their laser, stromal cuts showed 5 to 20-μ-wide zones of damage at the cut edge. At lower fluences, incisions could not be made, and only surface damage was observed. Loertscher et al. also used a multiline, HF laser to ablate cornea [24]. This group found 10–15 μm of damage near the top of corneal cuts and 1–2 μm of damage at the base of the incisions using 200-ns-long pulses and fluences from 0.7 to 2.3 J/cm^2. The HF laser emits at several wavelengths between 2.74 and 2.96 μm. It is known that the optical penetration depth of 2.74-μm radiation ($1/\alpha \approx 3.7$ μm) is almost five times greater than at the 2.94-μm peak ($1/\alpha \approx 0.79$ μm) [10–12]; thus thermal damage may not be minimized using the multiline HF laser. The uncertain effects of the multiline HF laser were avoided by Stern et al., who used a Raman-shifted Nd:YAG laser emitting 8-ns-long pulses of either 2.92 or 2.80-μm radiation [26]. Again, approximately 1.5 μm of uniform damage was noted at the base and as much as 10 μm of damage was noted near the top of ablation craters. Peyman and Katoh investigated the use of Q-switched and normal-spiking-mode Er:YAG laser radiation to ablate a variety of ocular structures [27]. However, their paper offers little discussion of irradiation parameters and almost no discussion of the results.

We present results that are in substantial agreement with those of the above researchers but differ on some important aspects. Furthermore, the experiments cover a wide range of fluences, use two significantly different pulse durations, include both soft and hard tissues, and document the effects of a reliable, relatively inexpensive, solid-state laser. Reported is the ablation of in vivo skin and in vitro cornea, bone, and aorta using a flashlamp-pumped Er:YAG laser emitting 2.94-μm radiation. The Er:YAG laser typically emits radiation in the normal-spiking mode, in which the output consists of a train of 1-μs-long pulses. However, we expected that a single pulse less than 1 μs in duration would be needed to minimize the zone of thermally-damaged tissue. To confirm this expectation, the Er:YAG laser was Q-switched to produce an approximately 90-ns-long [full width at half-maximum (FWHM)] pulse. Each tissue was ablated with both normal-spiking-mode and Q-switched pulses. The zone of thermally-altered tissue at the cut edge was quantified histologically using light microscopy. The results are explained using a simple model.

MATERIALS AND METHODS

An Er:YAG laser (Schwartz Electro-Optics, Concord, MA; model ER3000) was used in both the normal-spiking mode and the Q-switched mode to ablate guinea pig skin and bone, and bovine aorta and cornea. In the normal-spiking-mode, the Er:YAG laser emits approximately twenty 1-μs-long micropulses in an approximately 200-μs-long macropulse envelope. Using a rotating-mirror Q-switch, 90-ns-long (FWHM) pulses are emitted [5].

The 2.94-μm radiation emitted by the Er:YAG laser was attenuated with glass microscope slides and focused through an 8-in.-focal-length BaF_2 lens onto the tissue surface. The diameter of the beam at the tissue surface was determined by measuring the energy transmitted through a 10-μm-diameter aperture (Optimation, Windham, NH) that was stepped through the attenuated focus of the beam. In the normal-spiking mode, the Er:YAG laser was operated multimode, and the beam profile was uniform ± 10% over a diameter of 1.1 mm [5,28]. Q-switched, the laser

TABLE 1. Irradiation Parameters Used for Er:YAG Laser Ablation of Soft and Hard Tissues

Mode	Fluence/ pulse (J/cm^2)	Number of pulses	Rep rate (Hz)	Spot size (mm^2)
Q-switched	0.5–10	1–100	1	0.14
Normal mode	4–81	1–50	2	0.95

emitted a TEM_{00} mode beam with a 420 μm diameter at the tissue surface, as measured at the $1/e^2$ points [5]. The fluence per pulse was calculated from the pulse energy, as measured with a joulemeter (Gentec, model ED-200), and the measured spot diameter. The energy delivered per pulse was regulated by placing glass microscope slides in the beam path; each slide attenuates approximately 38%. Using attenuators to regulate energy delivery, as opposed, for example, to changing the bank voltage, means the irradiated spot was of constant diameter throughout the fluence range. Table 1 gives the irradiation parameters for the ablation experiments.

For the in vivo experiments, healthy guinea pigs (Hartley strain) were shaved with an electric razor and warm wax-epilated 24 hr prior to all irradiations using a 4:1 rosin:beeswax mixture. The guinea pigs were anesthetized with xylazine (5 mg/kg), ketamine (35 mg/kg), and atropine (40 μg/kg) prior to both epilation and laser irradiation. The above in vivo experiments were repeated using in vitro bovine aorta and cornea obtained directly from a slaughterhouse and guinea pig parietal bones and scapulas obtained immediately after sacrificing the guinea pigs with an anesthetic overdose of sodium pentabarbitol. All in vitro tissues obtained from the slaughterhouse were wrapped in plastic to inhibit desiccation and refrigerated; the tissue was then warmed to room temperature for use within 48 hr post-mortem. The guinea pig bones were used immediately post-mortem. Immediately after irradiation, each ablation site was observed grossly. Some sites were photographed using a 35 mm camera with a macrolens. All other sites were immediately biopsied. Each biopsy specimen was fixed in formalin, routinely processed, and stained with hemotoxylin and eosin. Routine processing of the bones included decalcification in 10% nitric acid.

RESULTS

The gross and histologic effects of the Er:YAG laser ablation of in vivo guinea pig skin and in vitro guinea pig bone and bovine cornea and aorta were investigated. Grossly, the only lesions that demonstrated charring were those created in bone with low fluence (i.e., less than 15 J/cm^2) normal-spiking-mode pulses. All other lesions failed to demonstrate charring. Approximately 80% of the in vivo skin lesions were hemorrhagic. This observation must, however, be considered in light of the hypotensive and hypothermic effects of anesthesia and epilation that decrease dermal blood flow; with normal dermal perfusion, more hemorrhaging might be seen.

The gross appearance of the lesions created in the aorta was markedly different from that seen in the other tissues (Fig. 1). In particular, the aortic lesions created by high-fluence, normal-spiking-mode irradiations were consistently elliptical, with the long-axis of the ellipse oriented circumferentially. The orientation of the ellipse was independent of the orientation of the aorta relative to the beam and therefore not a result of any indiscernible asymmetry in the beam. Tangential sections of the ablation craters produced by high-fluence, normal-mode irradiations indicate that the long axis of the elliptical lesion is parallel to the circumferentially oriented elastin fibers (Fig. 4D). Low-fluence (5 J/cm^2) aortic cuts were circular. There was a smooth transition between the high-fluence (80 J/cm^2) and low-fluence (5 J/cm^2) cuts. Elliptical cuts were not seen in any other tissues at any fluence and were not seen with any Q-switched irradiations.

On histologic examination the width of the damage zone was found to vary; thus, for each tissue the range of observed damage was tabulated (Table 2). In all tissues, the width of the damage zone at the edge of incisions made with Q-switched pulses was smaller.

In skin, ablation craters created with normal-spiking-mode pulses were bordered by a zone of altered tissue. This zone, typically 10–40 μm in width at fluences <25 J/cm^2, is characterized by increased hematoxylin staining of the collagen, loss of fibrillar appearance of the collagen, and thickening of the collagen fibers (Fig. 2A). Microscopic examination of the tissue sections using polarized light confirms that the only collagen that lacks birefringence is that collagen characterized by abnormalities in staining and morphology. Wider zones of damage (e.g., 50–100 μm) are observed at the highest fluence (88 J/cm^2). However, in contrast to the aorta and cornea, where tissue tearing is light-microscopically apparent, no tearing is observed in skin. In general, the epi-

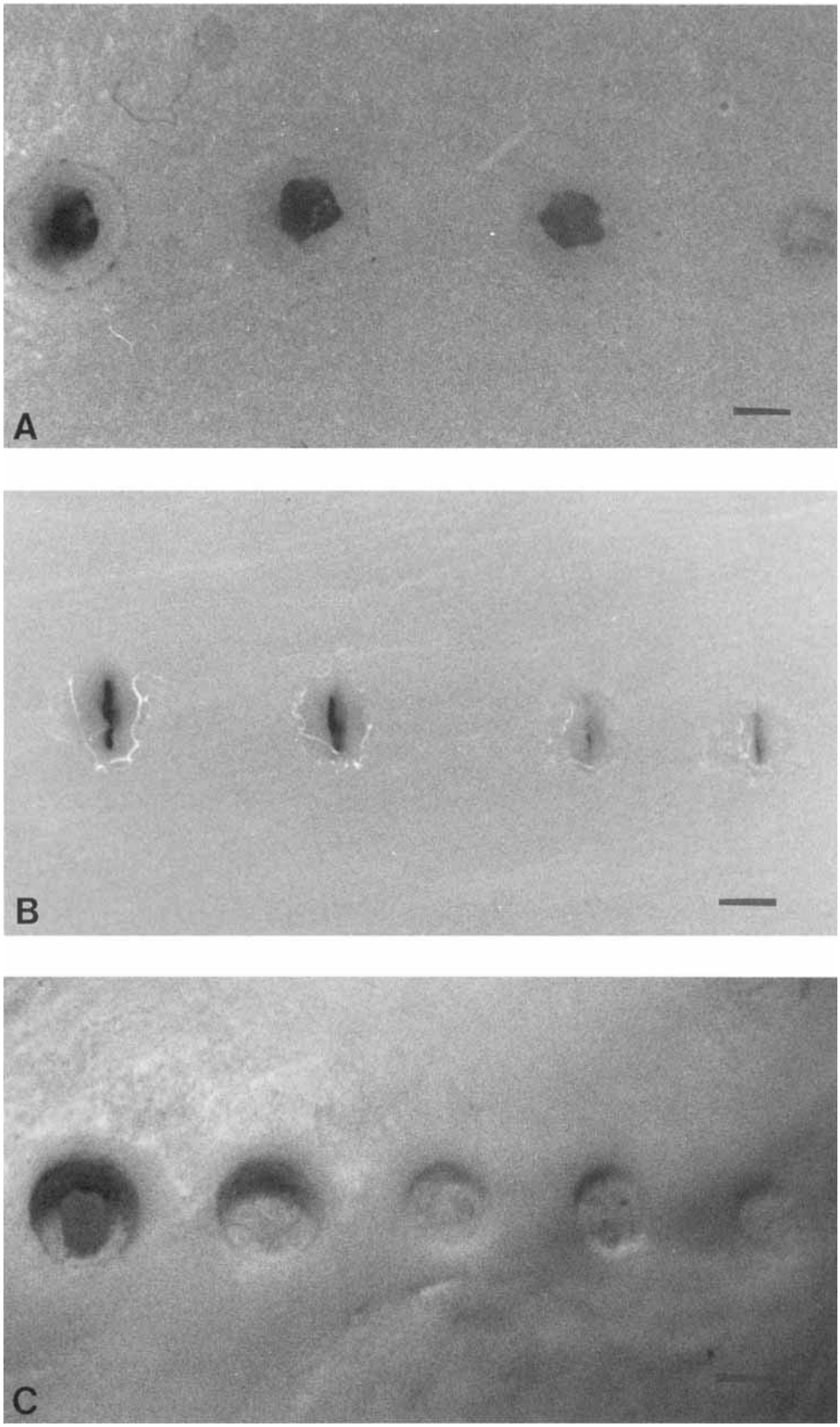

Fig. 1. Photographs of the ablation craters produced in skin **(A)**, aorta **(B)**, and bone **(C)**. All ablation craters were produced with the normal-spiking-mode Er:YAG laser at 81 J/cm^2 with a 1.1-mm-diameter spot. The number of pulses delivered is (from left to right): for skin, 20, 10, 5, and 1; for aorta, 8, 4, 2, and 1; and for bone, 14, 10, 6, 3, and 1. Bar = 500 μm.

TABLE 2. Width of the Damage Zone (μm) at the Bottom of the Ablation Crater Created With the Er:YAG Laser*

Tissue	Q-switched	Normal-spiking mode
Skin	5–10	10–50
Cornea	5–10	10–50
Aorta[a]	5–10	10–20
Bone	5–10	10–15

*At fluences greater than approximately 25 J/cm^2 wider zones of damage were noted in the soft tissues (see text).
[a]Collagen damage is reported; damage to elastin fibers could not be appreciated.

dermis demonstrates less damage than the dermis. This result may be an indication that the denaturation of epidermal cells requires higher temperatures for longer periods of time than the denaturation of collagen fibers. Alternatively, hematoxylin and eosin staining may not clearly differentiate normal and thermally-altered epidermal structures. The ablation craters created with the Q-switched pulses are similar to the craters created with normal-spiking-mode pulses; however, the zone of light-microscopically-apparent damage in the dermis is slightly thinner, only 5–10 μm in width, at the edge of the craters produced with the Q-switched pulses (Fig. 2B). With Q-switched pulses, there is no indication that damage varies over the range of fluences examined. Although damage zones as thin as 1–2 μm in width were observed, this finding could not be made consistently.

In cornea, normal-spiking-mode, high-fluence irradiations caused histologically apparent tears in the tissue. Figure 3A shows a cut produced in bovine cornea by three pulses at 80 J/cm^2; note the tears at the lateral edges of the ablation crater. Along the length of each tear is 10–20 μm of thermally-altered tissue; the zone of thermally-altered tissue immediately at the edge of the cut is 25–75 μm wide. At lower fluences (<25 J/cm^2), the zone of damage is typically 20 μm wide; the range is 10–50 μm (Fig. 3B). When Q-switched, the Er:YAG laser created corneal incisions that lacked evidence of tissue tearing; the zone of thermally-altered tissue is 5–10 μm wide (Fig. 3C).

In the aorta, as in the cornea, normal-spiking-mode, high-fluence (70 J/cm^2) irradiations created lesions with rough, undulating walls and collagen fiber damage that typically extends 50–100 μm from the cut edge. Furthermore, there are apparent separations in the tissue that extend up to 400 μm from the cut edge (Fig. 4A); these tears are demarcated by thermally altered collagen. At lower fluences (<25 J/cm^2), the edge of craters produced by normal-spiking mode pulses is characterized by smooth straight walls and 10–20 μm of thermal damage to the collagen fibers (Fig. 4B). No light-microscopically-apparent damage to the elastin fibers could be appreciated. With Q-switched pulses, collagen fiber damage extends only 5–10 μm from the cut edge (Fig. 4C), and no tissue tearing was noted.

High-fluence irradiations easily ablate bone and leave little thermally-damaged tissue at the cut edge (Table 2 and Fig. 5). The width of the damage zone is the same for both the parietal bone and the scapula. At lower fluences, e.g., less than 15 J/cm^2 normal-spiking mode, the first few pulses easily ablate bone; however, after approximately 50 pulses, the ablation rate is subjectively decreased, and charring of the surface is clearly evident. After approximately 200 pulses ablation ceases, presumably because of desiccation [28].

DISCUSSION

An Er:YAG laser, emitting at the 2.94-μm peak of the water absorption band, was used in both the Q-switched mode (90-ns-long pulses) and the normal-spiking mode (200-μs-long pulse trains) to ablate skin, cornea, aorta, and bone. The gross and histologic damage to tissue at the ablation crater edge was studied.

The results support a previous finding that the extent of thermal alteration varies from tissue to tissue [9]. In particular, the Er:YAG laser radiation does not appear to damage elastin fibers at the edge of the ablation crater in aorta, whereas collagen alteration is found as deep as 100 μm into the tissue (Fig. 4). The observed layering of damaged and undamaged tissue is felt to be caused by a difference in the thermodynamic denaturation properties of the tissue components.

The results also support the prediction that a single, short pulse of radiation can reduce residual thermal damage. A simple damage model based upon a thermal relaxation time, τ_R, given by

$$\tau_R \approx (1/\alpha)^2/4\kappa$$

where α is the absorption coefficient and κ is the thermal diffusivity of the tissue (typically 1.3×10^{-3} cm^2/s [29]), leads to the prediction that a pulse duration less than τ_R is needed to mini-

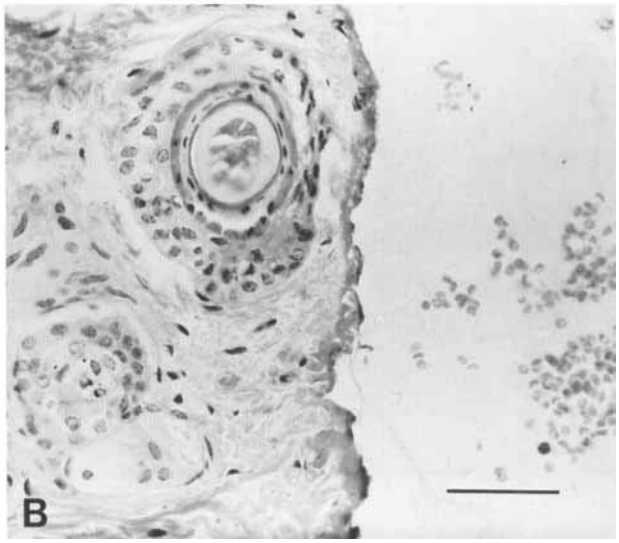

Fig. 2. **A:** Photomicrograph of guinea pig skin ablated by the normal-spiking-mode Er:YAG laser. An approximately 50-μm-wide zone of thermally-damaged collagen is seen at the base of the ablation crater. Irradiation conditions: 25 J/cm^2, 8 pulses, 2 Hz. Bar = 50 μm. **B:** Photomicrograph of guinea pigskin ablated by the Q-switched Er:YAG laser. A 5–10-μm-wide zone of damaged collagen is seen at the edge of the ablation crater. Irradiation conditions: 0.5 J/cm^2, 100 pulses, 1 Hz. Bar = 50 μm.

mize damage. We have previously shown that if the laser pulse duration was suitably short, then the zone of thermal damage at the edge of a CO_2 laser cut is typically 50 μm wide in a collagen-based tissue such as skin or cornea [9]. The results of the Er:YAG laser study also support the hypothesis that by using pulses shorter in duration than τ_R the zone of thermal damage is limited.

Two simple models exist that can be used to predict the width of thermally-damaged tissue left by short pulses of ablative laser radiation. The major assumption in these models is that there is a threshold amount of energy deposited at the base of the ablation crater. All tissue that receives more than the threshold amount of energy is ablated; nonablated tissue is thermally damaged if the energy that is deposited in that tissue heats the tissue above some critical value, e.g., 65°C for collagen-based tissues such as skin and cornea.

The first model, based upon Beer's law, predicts damage solely from the energy distribution at the end of the short laser pulse (Fig. 7). The depth of damage, D_d, is given by

$$D_d = (1/\alpha)\ln[F_{th}\alpha/(T_c - T_0)\rho c]$$

where F_{th} is the threshold fluence for ablation and therefore the energy deposited at the surface of the nonablated tissue, T_c is the critical temperature for the denaturation of the tissue, T_0 is the preirradiation tissue temperature, and ρc is the volumetric specific heat of the tissue [9]. As shown in Table 3, using this model approximately 3 μm of damaged tissue is expected at the base of a crater produced with a Q-switched Er:YAG laser pulse.

The second model considers thermal diffusion in a simple way. It is assumed that all of the energy left in the tissue at the end of the pulse is distributed in the tissue uniformly (Fig. 7). The height of the energy distribution is equal to the energy required to cause tissue denaturation. Thus

$$D_d = F_{th}/(T_c - T_0)\rho c.$$

As shown in Table 3, using this model one predicts 15 μm of damage. Because the second model puts all of the residual thermal energy into the tissue uniformly, the second model predicts an upper limit on the zone of thermal damage to be left by a short pulse of ablative radiation. The results of the Q-switched Er:YAG laser experiments indicate damage zones wider than given by the first model and thinner than predicted by the second model.

Both models neglect the dynamics of the ablation process, which require inclusion of ablative cooling of the tissue after the end of the pulse [30]

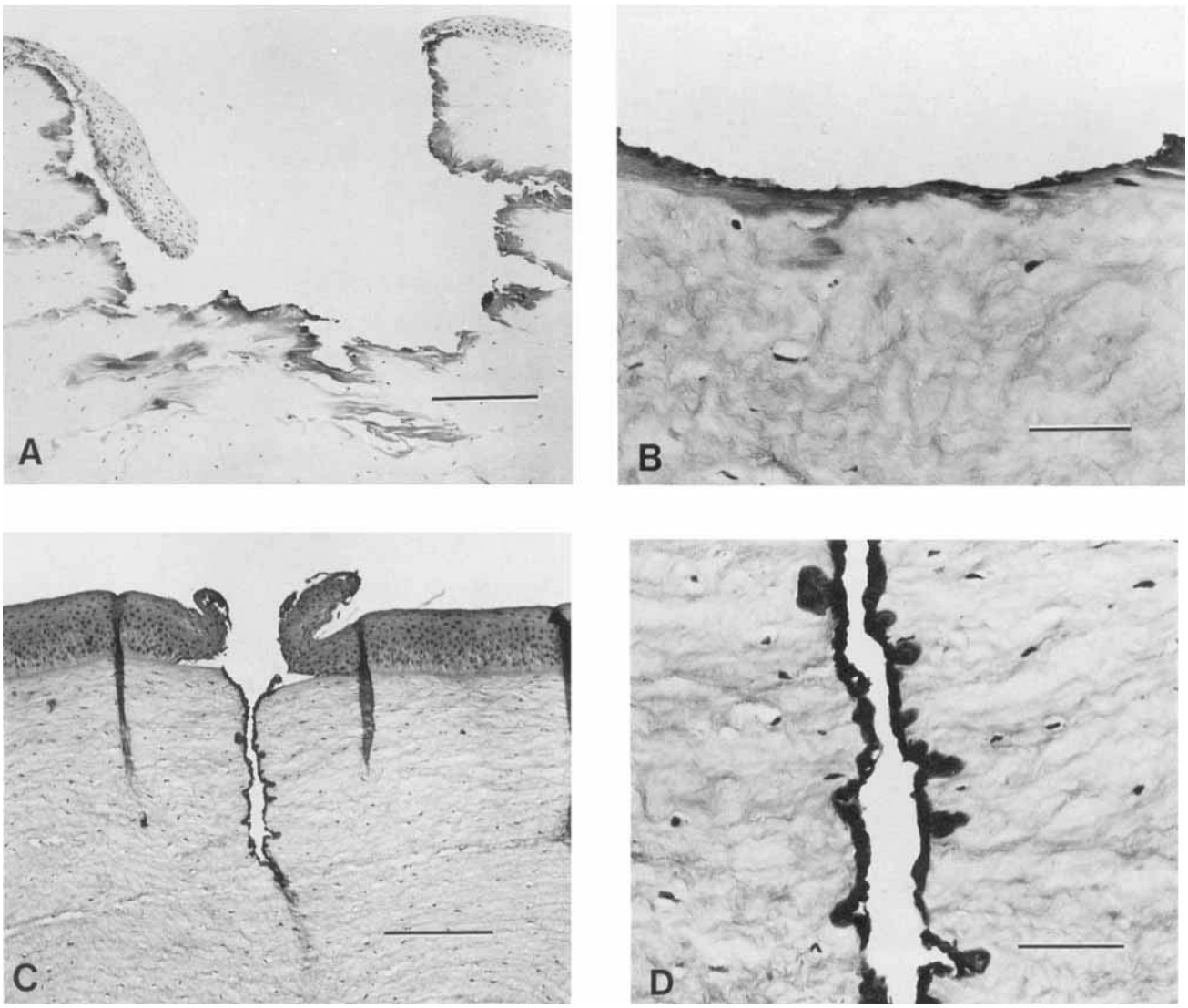

Fig. 3. **A:** Photomicrograph of bovine cornea ablated by the normal-spiking-mode Er:YAG laser. At high fluence the tissue appears shattered, and the tears seen at the ablation crater edge demonstrate thermally-altered tissue. The damage zone immediately at the crater edge is 20–60 μm wide. The appearance of "tongues" of corneal epithelium extending into the crater is common and without apparent explanation. Irradiation conditions: 80 J/cm^2, 3 pulses, 2 Hz. Bar = 200 μm. **B:** Photomicrograph of bovine cornea ablated by the normal-spiking-mode, Er:YAG laser. In contrast to high-fluence irradiations, at lower fluences the damage zone is much thinner, in this case 15–25 μm wide, and tears are not seen. Irradiation conditions: 22 J/cm^2, 3 pulses, 2 Hz. Bar = 50 μm. **C and D:** Photomicrograph of bovine cornea ablated by the Q-switched Er:YAG laser; the damage zone is less than 10 μm wide. Irradiation conditions: 1 J/cm^2, 60 pulses, 1Hz. C, bar = 200 μm; D, bar = 50 μm.

as well as the time-temperature dependence of the denaturation process as given by the Arrhenius integral [31,32]; thus, even the first model may overpredict the width of the thermal damage zone. Either post-pulse cooling or Arrhenius integral considerations can explain why zones of damage thinner than predicted by the Beer's law-based model have been reported. In these reports [24,26], it was found that very thin zones of damage were seen only at incident fluences near the threshold fluence for ablation. More sophisticated modeling (e.g., finite difference and finite element models) will likely consider the role of post-pulse thermal diffusion, post-pulse ablative cooling, and the time-temperature dependence of the damage process and thus provide a more detailed explanation for the fluence dependence of the width of the damaged zone.

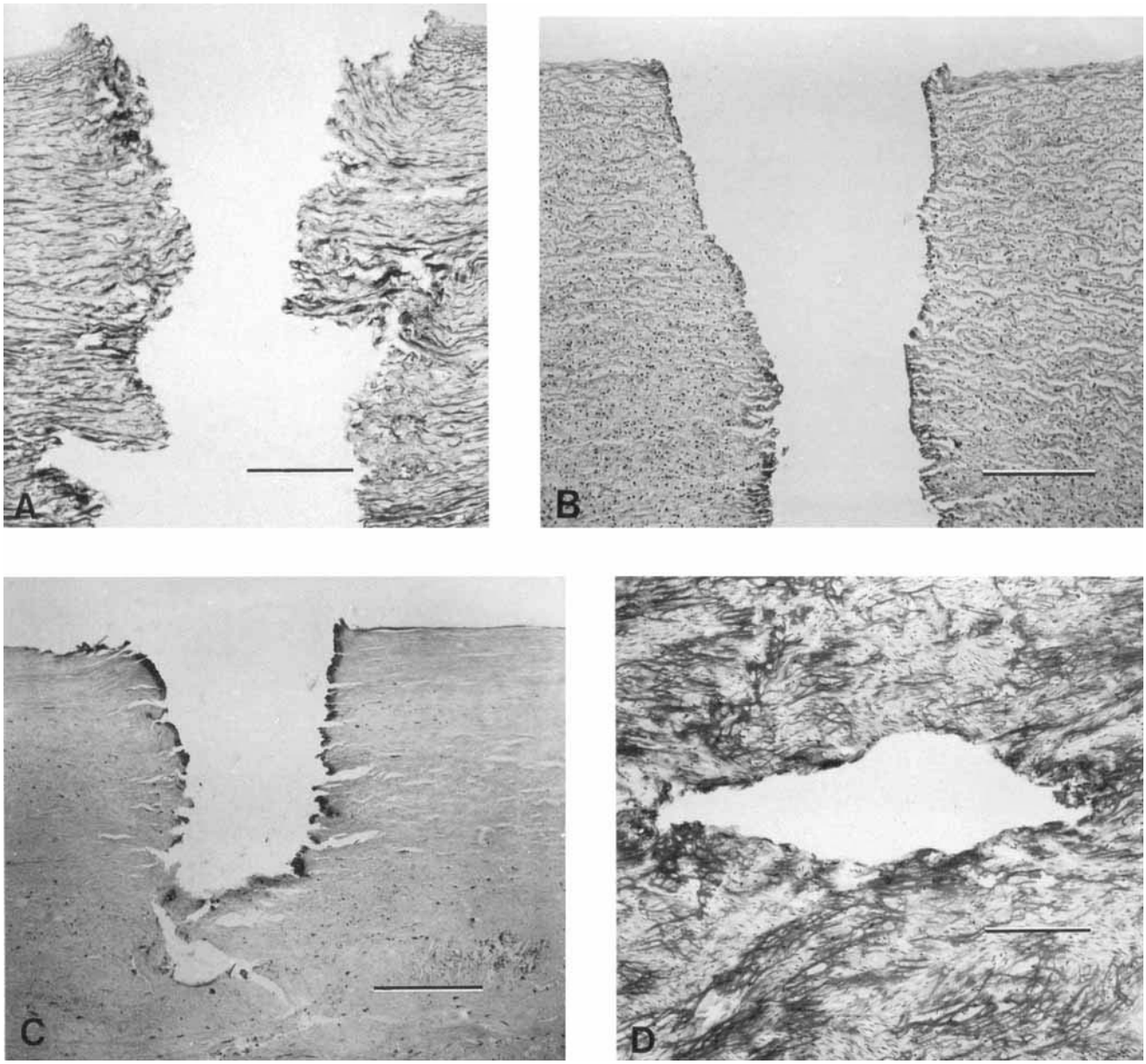

Fig. 4. **A:** Photomicrograph of bovine aorta ablated by the normal-spiking-mode Er:YAG laser. Note the ragged edges produced by the high-fluence irradiation. Damage to residual tissue is limited to the collagen fibers. Irradiation conditions: 70 J/cm^2, 2 pulses, 2 Hz. Bar = 200 μm. **B:** Photomicrograph of bovine aorta ablated by the normal-spiking-mode Er:YAG laser. At low fluences the walls of the crater are relatively smooth, and the damaged collagen zone is 10–20 μm wide. Irradiation conditions: 3 J/cm^2, 27 pulses, 2 Hz. Bar = 50 μm. **C:** Photomicrograph of bovine aorta ablated by the Q-switched Er:YAG laser. The damaged collagen zone extends 5–10 μm from the edge of the crater. Irradiation conditions: 6 J/cm^2, 100 pulses, 1 Hz. Bar = 50 μm. **D:** Photomicrograph of bovine aorta ablated by the normal-spiking-mode Er:YAG laser, tangential section. Note that the circumferentially oriented elastin and collagen fibers generally run parallel to the long axis of the elliptically shaped ablation crater produced by the high-fluence irradiation. Irradiation conditions: 70 J/cm^2, 2 pulses, 2 Hz. Bar = 50 μm.

The interpretation of the normal-spiking-mode data is less straightforward. If each 1 μs long micropulse is above the threshold fluence for ablation and acts independently, one might expect thermal damage to be the same as for the Q-switched case. Using an optical pump-probe technique, it has been shown that each micropulse can ablate tissue and eject a separate bolus

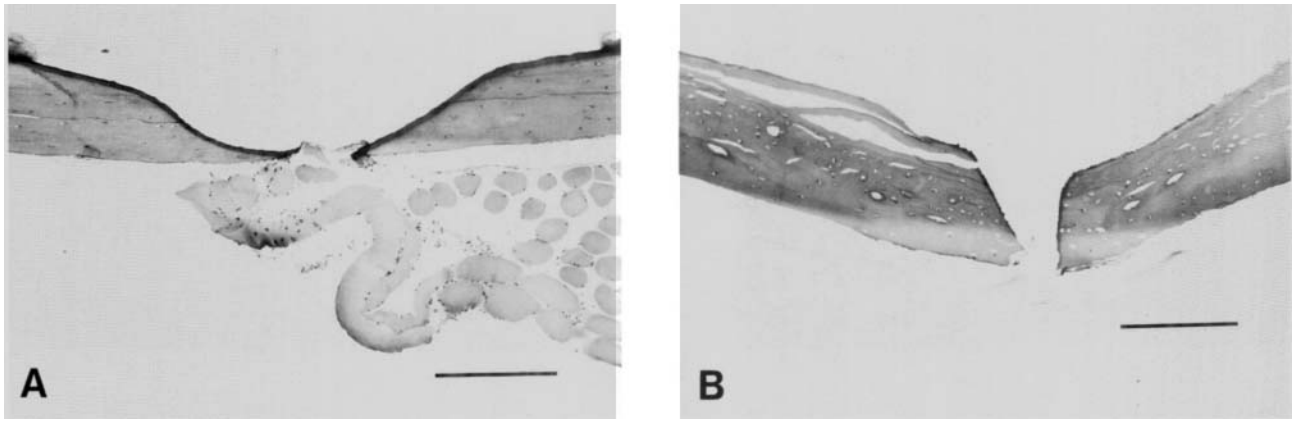

Fig. 5. **A:** Photomicrograph of guinea pig scapula ablated by the normal-spiking-mode Er:YAG laser. Damage to the bone extends 10–15 μm from the edge of the ablation crater. Irradiation conditions: 11 J/cm^2, 8 pulses, 2 Hz. Bar = 200-μm. **B:** Photomicrograph of guinea pig scapula ablated by the Q-switched Er:YAG laser. Damage to the bone extends 5–10 μm from the edge of the ablation crater. Irradiations conditions: 1 J/cm^2, 54 pulses, 1 Hz. Bar = 200 μm.

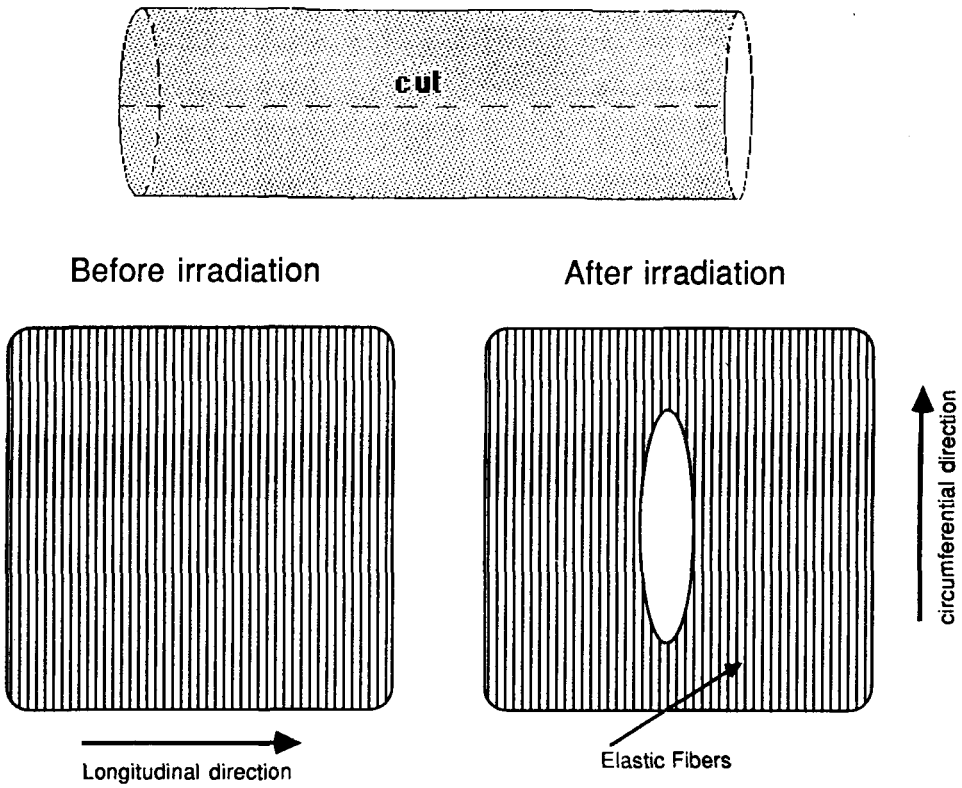

Fig. 6. Schematic representation of the high-fluence Er:YAG laser ablation of aorta. Er:YAG laser ablation of aorta appears to break weak links between strong elastic fibers.

of tissue [5]; thus each micropulse may act independently. However, in general, the damage left by normal-spiking-mode irradiations is more extensive than that left by Q-switched irradiations. Furthermore, the creation of elliptical craters in aorta by ablative laser pulses has not previously been reported. Given that the long axis of the ellipse was always in the circumferential direction, it appears that the shape of the crater is solely a function of tissue properties, as indicated in Figure 6. Histologic evidence also indicates the tearing of aortic tissue. Figure 3 shows that mechanical tissue separation effects were also observed in cornea, in which there is a lamellar nature to the

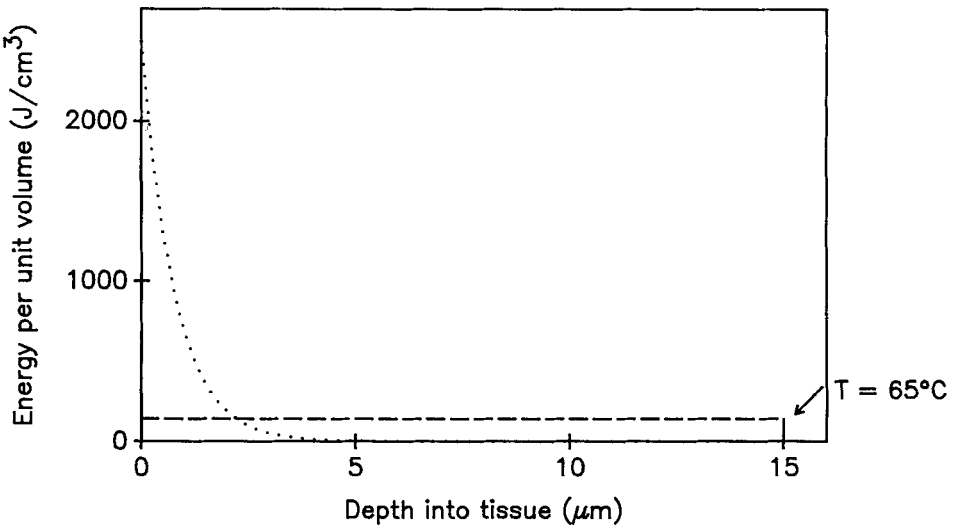

Fig. 7. Energy per unit volume vs. depth into the tissue. According to Beer's law, the energy deposited per unit volume decreases exponentially into the tissue (α = 13,000 cm^{-1}); thus the tissue within the first 3 μm of the tissue surface experiences an initial temperature (T) rise to above 65°C. If one considers a uniform distribution of the initially deposited energy, then 15 μm of tissue is heated to 65°C.

TABLE 3. Width of the Thermal Damage Zone as Predicted From Two Simple Models

Tissue parameters:	
α = 9,000 cm^{-1}	
F_{th} = 0.25 J/cm^2	
T_c = 65°C	
T_0 = 25°C	
ρc = 4.18 J/cm^3 °C	
Beer's law without thermal diffusion:	D_d = 3 μm
Thermal diffusion considered:	D_d = 15 μm

orientation of the collagen fibers [33]. In particular, there appears to be separation of the corneal lamella by breakage of the weak bonds between the strong collagen-based layers. The apparent thermal alteration of the tissue at the edges of both the corneal tears and the aortic tears, coupled with the consistent occurrence of tearing only during high-fluence irradiations, is evidenced that this tearing was caused by the ablative pulse and is not an artifact of tissue processing or stress-relaxation in the tissue after irradiation.

The results are consistent with the following proposed mechanism: the ablation of tissue by 2.94 μm radiation is an explosive process driven by the rapid heating, vaporization, and subsequent high-pressure expansion of irradiated tissue. This mode of ablation is not unique to 2.94-μm radiation; explosive material removal has been reported at 193 nm [34–37], 248 nm [34,37], 488 nm [38], 1.06 μm [39,40], and 10.6 μm [39,40]. While the penetration of more than 1 mm of tissue by a single 200-μs-long pulse would not be expected on the basis of a simple Beer's law blow-off model, it is not surprising in the context of a dynamic model in which material is removed during the pulse. Zwieg et al. have discussed one such model and presented measurements of Er:YAG laser ablation of gels to depths of almost 3 mm in a single pulse [41]. Furthermore, a simple Beer's law model does not account for as much as 100 μm of damage at the crater edge. The results are consistent with a dynamic picture in which 2.94-μm radiation penetrates far deeper into the tissue than the estimated 1-μm optical penetration depth.

In a dynamic model, material that is heated by the beginning of the pulse can be removed during the pulse, thus clearing a path for radiation at the end of the pulse to be deposited deeper within the tissue. High-speed photography suggests that such "burrowing" occurs during the normal-spiking-mode Er:YAG laser ablation of gelatin, a model system for tissue [41]. Second, vaporized material must not absorb the beam substantially. Water vaporized by the pulse has a much lower 2.94-μm optical absorption coefficient than liquid water. Statistical models exist that allow calculation of the 2.94-μm absorption coefficient in vapor water; calculations suggest that at 100 atmospheres, 3,000°K, the absorption coefficient, α, is approximately 2.7 cm^{-1} [42], i.e., $1/\alpha \approx 3.7$ mm.

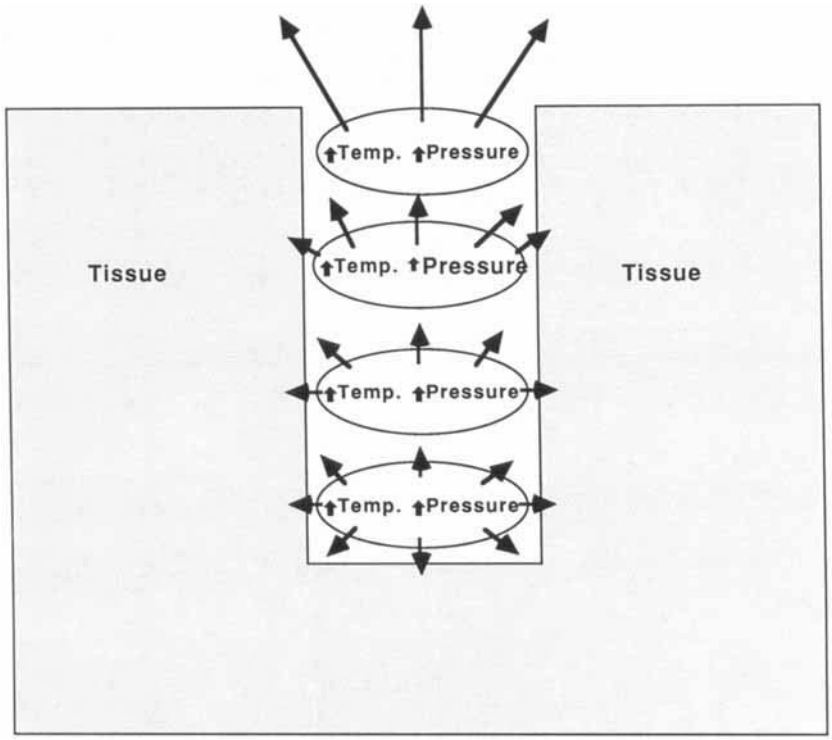

Fig. 8. Vaporization of water near the tissue surface allows 2.94-μm radiation to penetrate more deeply within the tissue. Tissue at the surface readily escapes. The tissue heated at depth cannot leave the ablation site until the tissue above leaves. Nonablated tissue along the side and at the base of the crater is heated by the hot gases and if the gas pressure is high enough tissue tearing can occur.

At lower temperatures and pressures the $1/\alpha$ depth is even greater. By comparison, the optical absorption coefficient of pure water at 2.94 μm is approximately 13,000 cm^{-1}, i.e., $1/\alpha \approx 0.79$ μm [10]. Thus, once vaporized, the tissue at the surface no longer absorbs a significant percentage of 2.94-μm radiation; this radiation is therefore absorbed deeper in the tissue.

Independently of the details of how radiation penetrates more deeply into the tissue than a Beer's law model would predict, we suggest that high-temperature, high-pressure gases develop at the site of absorption (Fig. 8). These high-pressure gases cause breakage of the weak bonds that hold together the circumferentially-oriented elastin and collagen fibers in aorta and the lamella in cornea. In addition, liquefied tissue can exert radial forces on the walls of the cut [41]. The thermal damage observed at the edge of the tears suggests that the gases formed during ablation are both hot, therefore capable of thermally damaging tissue, and at high pressure, therefore capable of tearing tissue. Furthermore, when material particularly deep within the tissue is vaporized, e.g., during high-fluence, normal-spiking-mode ablation, it cannot easily expand. It is, therefore, likely that the vaporization temperature of the tissue rises well above 100°C, and thermal alteration of the surrounding, nonablated tissue increases. This mechanism would also explain why the width of the damage zone is as much as 100 times the estimated 1 μm optical penetration depth of the 2.94-μm radiation. In addition, some liquefied tissue may remain at the walls of the crater after the pulse; the heat in this liquefied tissue may diffuse into the unirradiated tissue, leading to further residual thermal damage [41].

For Q-switched pulses, which were lower fluence than the normal-spiking-mode pulses, a relatively shallow depth of tissue was vaporized, the confinement of the hot gases did not occur, and the crater walls were only minimally heated by the vaporized material as it left the tissue. Interestingly, other researchers using mid-infrared laser pulses shorter in duration than the 1 μs thermal relaxation time have reported 1–2 μm of damage at low fluence and 10 μm of damage at higher fluences (e.g., >1 J/cm^2) [24,26]. As with the normal-spiking-mode pulses, perhaps the confinement of larger volumes of heated tissue that

are produced at higher fluence leads to increased damage.

Similarly, at lower normal-spiking-mode fluences, because the depth of tissue ablated is small [28], the vaporized tissue can more easily expand into the low pressure (1 atmosphere) air. At high fluence, the depth of tissue ablation is large [28]; thus the hot, high-pressure gases produced deep within the tissue do not "see" a low-pressure region in which to escape. Instead, these gases "see" only the hot, high-pressure gases above and the tissue laterally and below. The high-pressure gas produced at depth expands into the region of least impedance: for the cornea, that region is between the collagen lamella; for the aorta, this expansion leads to breakage of the weak bonds between the strong, circumferentially-oriented fibers. For the dermis, which has isotropically-oriented collagen fibers, the pressures generated in this experiment were apparently not great enough to separate the tissue; as a consequence, circular ablation craters were produced in skin, and histologic evidence of tissue tearing could not be found. Bone is even stronger than skin and also has relatively isotropic strength properties; thus circular craters without evidence of tearing were produced.

In conclusion, we have proposed that 2.94- μm radiation is deposited more deeply within tissue than the absorption coefficient for pure water would suggest. This in-depth absorption explains: 1) zones of residual thermal damage that increase greatly at high fluence; 2) tearing of tissue; and 3) large etch depths per pulse [21,28].

ACKNOWLEDGMENTS

We would like to thank Drs. Kevin Schomacker, Martin Prince, Glenn LaMuraglia, and Franz Hillenkamp for their many insightful discussions and Margo Goetschkes and Faith Caverly for their technical support. We would also like to thank Dr. Peter Moulton and Jeff Manni of Schwartz Electro-Optics for their help with the Er:YAG laser. This work was supported in part by the SDIO-MFEL Program under contract N00014-86-K-0117 and by the Arthur O. And Gullan M. Wellman Foundation.

REFERENCES

1. Goldman L, Rockwell J. "Lasers in Medicine." New York: Gordon and Breach, 1971.
2. Kamat BR, Carney JM, Arndt KA, Stern RS, Rosen S. Cutaneous tissue repair following CO_2 laser irradiation. J Invest Dermatol 1986; 87:268–271.
3. Hall RR. The healing of tissues incised by a carbon-dioxide laser. Br J Surg 1971; 58:222–225.
4. Olbricht SA, Stern RS, Tang SV, Noe JM, Arndt KA. Complications of cutaneous laser surgery. Arch Dermatol 1987; 123:345–349.
5. Walsh JT. Pulsed laser ablation of tissue: analysis of the removal process and tissue healing. Ph.D. Thesis, MIT Archives, Cambridge, MA, 1988.
6. Aron-Rosa DS, Boerner CF, Bath P, Carre F, Gross M, Timsit JC, True L, Hufnagel T. Corneal wound healing after excimer laser keratotomy in a human eye. Am J Ophthalmol 1987; 103:454–64.
7. Fry TL, Gerge RW, Botros SB, Fischer ND. Effects of laser, scalpel, and electrosurgical excision on wound contracture and graft "take." Plast Reconstruct Surg 1980; 665:729–731.
8. Munnerlyn CR, Koons SJ, Marshall J. Photorefractive keratectomy: a technique for laser refractive surgery. J Cataract Refract Surg 1988; 14:46–52.
9. Walsh JT, Flotte TJ, Anderson RR, Deutsch TF. Pulsed CO_2 laser tissue ablation: effect of tissue type and pulse duration on thermal damage. Lasers Surg Med 1988; 8: 108–118.
10. Hale GM, Querry MR. Optical constants of water in the 200-nm to 200-μm wavelength region. Appl Optics 1973; 12:555–563.
11. Robertson CW, Williams D. Lambert absorption coefficients of water in the infrared. J Opt Soc Am 1971; 61: 1316–1320.
12. Zolotarev MV, Mikhailov BA, Aperovich LI, Popov SI. Dispersion and absorption of liquid water in the infrared and radio regions of the spectrum. Opt Spectrosc 1969; 27:430–432.
13. Lane RJ, Linsker R, Wynne JJ. Ultraviolet-laser ablation of skin. Arch Dermatol 1985; 121:609–617.
14. Srinivasan R, Mayton-Banton V. Self-developing photoetching of poly(ethylene terephthalate) films by far-ultraviolet laser radiation. Appl Phys Lett 1982; 41:576–578.
15. Puliafito CA, Steinert RF, Deutsch TF, Hillenkamp F, Dehm EJ, Adler CM. Excimer laser ablation of the cornea and lens. Exp Studies Ophthalmol 1985; 92:741–748.
16. Pathak MA, Fitzpatrick TB, Parrish JA. Photosensitivity and other reactions to light. In Isselbaher KJ (ed): "Harrison's Principles of Internal Medicine," Ed 9. New York: McGraw-Hill, 1980, pp 255–262.
17. Wolbarsht ML. Laser surgery: CO_2 or HF. IEEE J Quantum Electronics 1984; QE-20:1427–1432.
18. Esterowitz L, Hoffman CA, Tran DC, Levin K, Strom M, Bonner RF, Smith P, Leon M, Ferrans V, Wolbarsht ML, Foulks GN. Advantages of the 2.94 μm wavelength for medical laser applications. In: "Technical Digest: Conference on Lasers and Electro-optics." Washington, DC: Optical Society of America, 1986, p. 122, paper TUL1.
19. Wolbarsht ML, Foulks GN. Corneal surgery with an Er:YAG laser at 2.94 μm. Lasers Surg Med 1986; 6:241.
20. Wolbarsht ML, Esterowitz L, Tran D, Levin K, Strom M. A mid-infrared (2.94 μm) surgical laser with an optical fiber delivery system. Lasers Surg Med 1986; 6:257.
21. Bonner RF, Smith PD, Leon M, Esterowitz L, Strom M, Levin K, Tran D. Quantification of tissue effects due to a pulsed Er:YAG laser at 2.94 μm with beam delivery in a

wet field via zirconium fluoride fibers. In: Katzir A, ed. "Optical Fibers in Medicine II" Proc. SPIE 1986; 713:2–5.
22. Nuss RC, Fabian RL, Sarkar R, Puliafito CA. Infrared laser bone ablation. Lasers Surg Med 1988; 8:381–391.
23. Nelson JS, Yow L, Liaw LH, Macleay L, Zavar RB, Orenstein A, Wright WH, Andrews JJ, Berns MW. Ablation of bone and methacrylate by a prototype mid-infrared erbium:YAG laser. Lasers Surg Med 1988; 8:494–500.
24. Loertscher H, Mandelbaum S, Parrish RK, Parel JM. Preliminary report on corneal incisions created by a hydrogen fluoride laser. Am J Ophthalmol 1986; 102:217–221.
25. Seiler T, Marshall J, Rothery S, Wollensak J. The potential of an infrared hydrogen fluoride (HF) laser (3.0 μm) for corneal surgery. Lasers Ophthalmol 1:49–60, 1986.
26. Stern D, Puliafito CA, Dobi ET, Reidy WI. Infrared laser surgery of the cornea: studies with a Raman-shifted Nd:YAG laser at 2.80 and 2.92 μm. Ophthalmology 1988; 95:1434–1441.
27. Peyman GA, Katoh N. Effects of an erbium:YAG laser on ocular structures. Int Ophthalmol 1987; 10:245–253.
28. Walsh JT, Deutsch TF. Er:YAG laser ablation of tissue: measurement of the ablation rate. Lasers Surg Med 9:327–337.
29. Bowman HF, Cravalho EG, Woods M. Theory, measurement, and application of thermal properties of biomaterials. Annu Rev Biophys Bioeng 1975; 4:43–79.
30. Rosen DI, Popper LA. Modeling of the laser induced ablation and thermal damage of biological tissue. SPIE 1989; 1064:(in press).
31. Hillenkamp F. Interaction between laser radiation and biological systems. In Hillenkamp F, Pratesi R, Sacchi CA (eds): "Lasers in Biology and Medicine," New York: Plenum Press, 1979, pp 37–68.
32. Henriques FC. Studies of thermal injury. Br J Surg 1947; 58:489–502.
33. Bloom W, Fawcett DW. "A Textbook of Histology," Ed 10. Philadelphia: W. B. Saunders Co., 1975, pp 921–923.
34. Puliafito CA, Stern D, Kreuger RR, Mandel ER: High speed photography of excimer laser ablation of the cornea. Arch Ophthalmol 1987; 105:1255–1259.
35. Dyer PE, Srinivasan R. Nanosecond photoacoustic studies on ultraviolet laser ablation of organic polymers. Appl Phys Lett 1986; 48:445–447.
36. Srinivasan R, Dyer PE, Braren B. Far-UV laser ablation of cornea: Photoacoustic studies. Lasers Surg Med 1987; 6:514–519.
37. Srinivasan R, Braren B, Seeger DE, Dreyfus RW. Photochemical cleavage of a polymeric solid: details of the ultraviolet laser ablation of poly(methyl methacrylate) at 193 and 248 nm. Macromolecules 1986; 19:916–921.
38. Prince MR, Deutsch TF, Shapiro AH, Margolis RJ, Oseroff AR, Fallon JT, Anderson RR. Selective ablation of atheromas using a flashlamp-excited dye laser at 465 nm. Proc Natl Acad Sci USA 1986; 83:7064–7068.
39. Paek UC, Zaleckas VJ. Scribing of alumina material by YAG and CO_2 Lasers. Ceramic Bull 1975; 54:585–588.
40. Gagliano FP, Paek UC. Observation of laser-induced explosion of solid materials and correlation with theory. Appl Optics 1974; 13:274–279.
41. Zweig AD, Frenz M, Romano V, Weber HP. A comparative study of laser tissue interaction at 2.94 μm and 10.6 μm. Appl Phys B 1988; 47:259–265.
42. Young JS. Evaluation of nonisothermal band model for H_2O. J Quant Spectrosc Radiat Transfer 1977; 18:29–45.